



## CFD Simulation on Permeability of Porous Scaffolds for Human Skeletal System

**Norhana Jusoh<sup>1,2,3\*</sup>, Amirul Azri<sup>1</sup>, Auni Nurhaziqah Mohd Noor<sup>1</sup>, Azizul Hakim Khair<sup>1</sup>, Azureen Naja Amsan<sup>1</sup>, Muhammad Husaini Amir Hussein<sup>1</sup>, Muhammad Syahmi Hafizi Abd Shukor<sup>1</sup>, Tariq Muhammad Aminuddin<sup>1</sup>, Adlisa Abdul Samad<sup>1</sup>**

<sup>1</sup>School of Biomedical Engineering and Health Sciences, Universiti Teknologi Malaysia, 81310 UTM Johor Bahru, Johor, Malaysia

<sup>2</sup>Medical Device Technology Center (MEDiTEC), Institute Human Centred Engineering (iHumen), Universiti Teknologi Malaysia, Skudai 81310, Johor, Malaysia.

<sup>3</sup>Bioinspired Device and Tissue Engineering Research Group, School of Biomedical Engineering and Health Sciences, Universiti Teknologi Malaysia, 81310 UTM Johor Bahru, Johor, Malaysia

\*Corresponding Author [norhana@utm.my](mailto:norhana@utm.my)

Received 28 October 2021; Accepted 24 January 2022; Available online 31 January 2022  
<https://doi.org/10.11113/humentech/v1n1.11>

### Abstract:

Human skeletal system provides the protection of all organs and supports the loads from various daily activities. Therefore, the main objective of bone scaffold is to have mechanical strength to support the load and have the permeability that will have mass fluid transfer to enhance the healing of defects. In this study, we simulated the permeability of hexagonal unit cells at different pore sizes (1.0 mm, 1.5 mm and 2.0 mm) and at different inlet velocities (0.001 mm/s, 0.5 mm/s and 1 mm/s) by using Computational Fluid Dynamic (CFD) in Ansys software. Our finding shows that pressure drop from inlet to the outlet of the unit cell's pore increased corresponding to the decreasing of pores diameter. In contrast, increasing the velocities has increased the pressure drop from inlet to the outlet. The pressure drop at 0.001 mm/s, 0.5 mm/s and 1mm/s inlet velocities were  $1.40 \times 10^{-4}$  Pa,  $7.02 \times 10^{-2}$  Pa and  $1.41 \times 10^{-1}$  Pa, respectively for 1.0 mm pore size. The gradual decreased of the pressure will give the cell and nutrient to be diffused to the inner part of the scaffold. We calculated the permeability for each unit cell, and it can be acceptable based on the upper limit of human bone permeability. The variation in velocities did not gave significant differences for the scaffold permeability. However, the different of pore sizes gave significant effect in the scaffold permeability. The permeability value at 0.001 mm/s for 1.0 mm, 1.5 mm and 2.0 mm pore size were  $2.900 \times 10^{-8}$  m<sup>2</sup>,  $4.863 \times 10^{-8}$  m<sup>2</sup> and  $8.529 \times 10^{-8}$  m<sup>2</sup>, respectively. By taking into accounts the pressure drop and permeability value, unit cell with 1 mm pore size is predicted to show a better performance in promoting cell growth due to the better flow characteristics in the scaffold. Permeability prediction will help in producing a functional bone scaffold that crucial in bone regeneration of the human skeletal system.

Keywords: Human skeletal; Bone scaffold; Hexagonal pore; Unit cell; Permeability

## 1. Introduction

The human skeletal system that consists of 206 bones is functioning in providing structure and protection for all organs as well as facilitates the movement between the joints and muscles [1]. The skeletal system has to support the

loads of various human's activities that contribute to injuries and disorders [1,2]. However, bone which consists of osseous tissue, bone marrow, endosteum, periosteum, cartilage, nerves, and vascular channels has ability in regenerating to adapt the loads that may cause tensile, compressive, or shear stresses on the bone tissue [1,2]. The repair and reconstruction of bone tissue has always been the highlight of tissue engineering [3]. For the past few decades, bone tissue engineering has recorded a significant improvement especially in creating bone substitutions which replaces autograft and allograft. In order to support the implementation of progenitor bone cells or any other biological components with the aim of stimulating new bone growth, the idea of creating a synthetic or partially synthetic scaffold is introduced [4].

One of the most challenging tasks for researchers nowadays is designing artificial scaffolds with tissue growth capability. This is because scaffold design is known as a complex process as it requires suitable selection and control of various parameters for example mechanical properties, biodegradation, biocompatibility, pore architecture, porosity, surface properties and most crucial one, the permeability [5]. Permeability is a parameter which measures quantitatively the capability of a porous medium to conduct fluid flow and it relies on the combination of porosity, pores size, orientation, tortuosity, and interconnectivity. In addition, permeability is vital for bone regeneration not only because bigger values are believed to enhance bone ingrowth [6] but also because insufficient values may induce the formation of cartilaginous tissue instead of bone [7,8].

The size of pore of porous scaffold also plays an important role in bone regeneration. One of the most obvious problems of porous implants that need to be addressed is optimization of the structure to promote osteogenesis. Quite a few studies have confirmed that the key parameter which affects bone regeneration is the pore size. One of the studies showed that the findings can be used in optimizing the porous scaffold architecture which can stimulate bone regeneration. The three-dimensional (3D) scaffold pore architecture is also an important design parameter, as it affects not only the mechanical properties but also the capability for cells to penetrate the scaffold and for nutrients, oxygen and waste products to diffuse through the scaffold [4]. Researchers has developed numerous studies on scaffolds permeability [9-11], and using permeability as a design tool have been focused on by a number of researchers. Porous scaffolds are three-dimensional polymeric porous scaffolds which are highly useful for tissue engineering. It contains a higher porosity and a homogeneous interconnected pore network [12]. It functions to give a support for any repair in human body. Some criteria must be considered in designing the scaffold which are biocompatibility, biodegradability, mechanical properties, proper architecture, and permeability. For biocompatibility, the term is referred to the cell attachment and proliferation which also involves a lack of toxicity and inflammatory reactions [13]. Next, biodegradability is considered as indispensable elements for engineering living tissues as they are used as temporary templates with specific mechanical and biological properties like native extracellular matrix (ECM). Good mechanical properties are needed and important because the mechanical properties will determine the ability of the scaffold to bear weight during the amelioration period. Other criteria to be considered in designing a bone scaffold that is proper architecture include the porosity and pore sizes, the diameter of the pore for the cell penetration or nutrients and waste transfer, and angiogenesis.

The porous scaffold is categorized to have a very complex process that requires an appropriate selection and control of multiple parameters including permeability. A permeability is related to the number of interconnecting pores that determines the ability of fluid flow inside a porous material to enhance the healing of defects. The scaffold permeability is a determinant factor as it plays a major role in the ability for cells to penetrate the porous media and for nutrients to diffuse [4]. It is considered as the main parameter for the microstructural design of the scaffolds since it contributes to the capability for waste removal and the supply of nutrients or oxygen. Not only that, but the diameter of the pores is also important since it may affect the permeability of the scaffolds. This is because the force and velocity that pass through the pore will be different each time which is due to the difference in the pore size of the pore in the bone scaffolds. To emphasize, one of the factors that may affect the permeability of the scaffolds is the diameter of the pores. The bone scaffold fabrication requires controlling multiple parameters involving biocompatibility, biodegradability, mechanical properties, proper architecture, and permeability. In this study, the team has emphasized one of the crucial parameters which are permeability. Permeability is related to the number of interconnecting pores, and it determines the ability of fluid flow inside a porous material [5]. Higher permeability has the disadvantages of high flow rate which causes washout of cells resulting in lower bone growth. The lower the permeability of the scaffolds, it will lead to low nutrient supply to cells which create hindrance for the growth of the bones [5]. Hence, there is always a range of desired permeability like that of natural bones found in different parts of the body. The desired range of the permeability is like natural bone which is  $(0.5 < k (10^{-8} \text{ m}^2) < 5)$  [5].

One of the factors that might be affecting the permeability of a bone scaffold is the pore size. The permeability for the bone scaffolds will differ when the pore sizes or the diameter of the pores are different. When the diameter of the pores is different, it will make a change to the thickness of the wall. The thickness of the wall will then determine whether the scaffolds are able to counter the force from the fluid pass through the scaffold. The permeability of the bone scaffolds can be determined from the diameter of pore scaffolds. This is due to the velocity of the fluid that passes through, which

is that different values of velocity will come out different force exerted to the wall of the scaffold. Lastly, the force exerted will determine the permeability of the bone scaffold. The prediction of scaffold permeability is one of important factor in designing a scaffold [14]. Therefore, in this study, we designed bone scaffold with different pore sizes by using SOLIDWORKS and we predicted the permeability for each scaffold by CFD simulation via Ansys Software.

## 2. Methods

In this experiment, the permeability of scaffold with different pore sizes have been obtained through Computational Fluid Dynamics (CFD) simulation in Ansys software. The experiment begins by designing scaffold unit cells in SOLIDWORKS software. Three different pore size of hexagonal shape were created with 1.0 mm, 1.5 mm and 2.0 mm respectively. Those design files were then imported to Ansys software by converting .sldprt files into .Iges files. Each scaffold unit cell design fluid flow model was created in the fluid flow (fluent) application. Figure 1 below shows the final design of the hexagonal unit cell with different pore sizes.

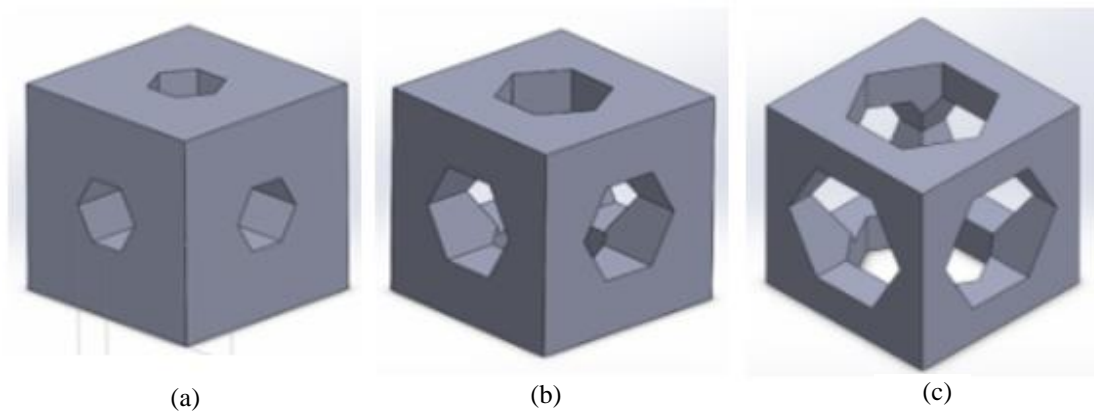


Figure 1. Hexagonal unit cell with pore size of (a) 1.0 mm, (b) 1.5 mm and (c) 2.0 mm

Based on hexagonal unit cell design, the corresponding fluid flow models of unit cells with different pore size, is shown in Figure 2.

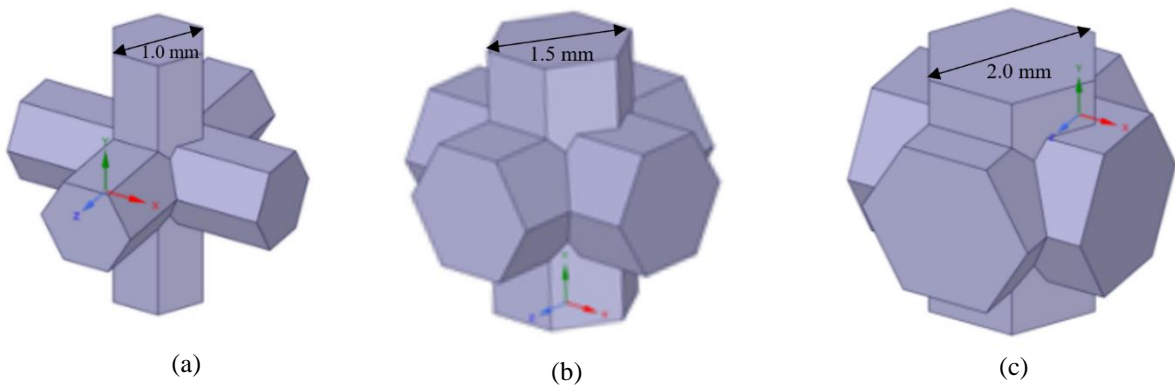


Figure 2. Fluid flow models of hexagonal unit cell with pore size (a) 1.0 mm, (b) 1.5 mm and (c) 2.0 mm

Before the analysis of CFD, fluid properties were inserted, and boundary conditions were defined. Once these conditions and properties were specified, the meshing was done, and the simulation was conducted. Pressure and velocity distribution for each scaffold unit cell designs were obtained, and these values were used to find scaffold’s permeability through Darcy’s formula, as shown in the equation below [5].

$$K = \vartheta_D \cdot \mu_D \cdot \left( \frac{L}{\Delta P_{i-o}} \right) \quad (1)$$

where,  $K$  = Permeability of unit cell;  $L$  = Length of fluid model;  $\Delta P_{i-o}$  = Pressure difference between inlet and outlet;  $\vartheta_D$  = Velocity at inlet; and  $\mu_D$  = Viscosity of the DMEM Fluid.

### 2.1 Scaffold model and fluid flow design

A unit cell with hexagonal pore share was created at different pore sizes of 1.0 mm, 1.5 mm and 2.0 mm. The dimension of the unit cell is 2.8 mm × 2.8 mm × 2.8 mm for all models. Once the design for each scaffold was completed, the CAD file was converted into .Iges files so that it can be imported to CFD software. Fluid flow models were obtained by tracing the volume of interest of the scaffold unit cells in the Ansys workbench software through the use of volume extract tools and selecting the edges found on the inside of the scaffold. Fluid flow models complimentary to the scaffold structure were created. For the fluid flow model, a few assumptions were made to ease the complexity of flow modelling and reduce the time for computational CFD analysis. Based on previous research, only one-unit cell of flow model per pore diameter size was used since its value represents the permeability of the entire scaffold [5]. We also assumed that the material of scaffold has an intrinsic property with uniform pore distribution.

### 2.2 Fluid properties parameters

Once Fluid Flow models were created, parameters for fluid properties were assigned before the simulation process. Fluid used is Dulbecco modified Eagle’s minimal essential medium (DMEM) at 1000 kg/m<sup>3</sup> density and 0.0015225 Pa.s viscosity. DMEM has almost twice the concentration of amino acids and four times the number of vitamins as EMEM, as well as ferric nitrate, sodium pyruvate, and some supplementary amino acids, which makes it ideal for tissue culture.

### 2.3 Boundary conditions

The inlet velocity applied at the top is varied between 0.0001 m.s, 0.5 mm/s and 1 mm/s, the pressure at outlet at the bottom was considered 0 and the other surfaces are considered fluid wall condition with no slip surface [5]. After applying those conditions, the simulation was performed, and the pressure drop across the unit cell was measured.

## 3. Results and Discussion

By using SOLIDWORKS software, three design of the scaffold models with different pore sizes which are 1.0 mm, 1.5 mm and 2.0 mm is successfully designed. By using ANSYS software, pressure distribution and velocity distribution for each unit cell at different velocities of 0.001 mm/s, 0.5 mm/s and 1mm/s were successfully obtained. Figure 3, 4 and 5 show the pressure distribution at different velocities for 1.0 mm, 1.5 mm and 2.0 mm, respectively.

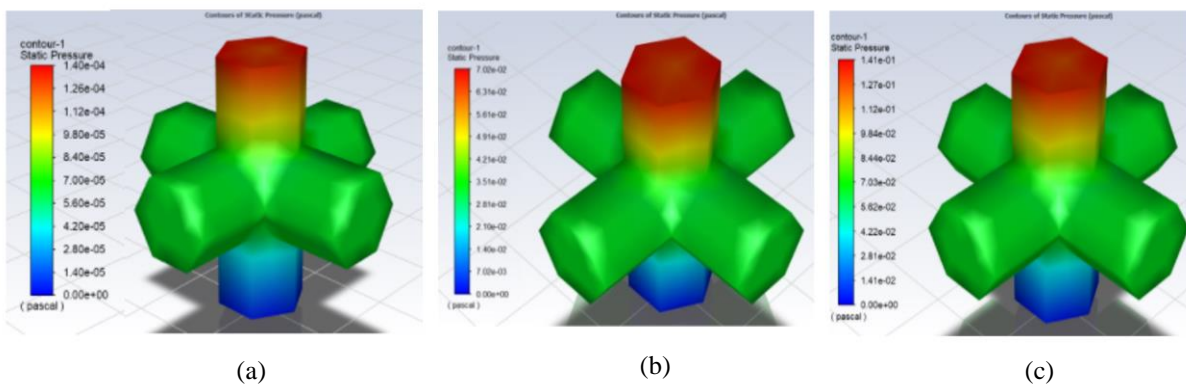


Figure 3. Pressure distribution of 1.0 mm hexagonal unit cell at different velocities (a) 0.001 mm/s, (b) 0.5 mm/s and (c) 1 mm/s

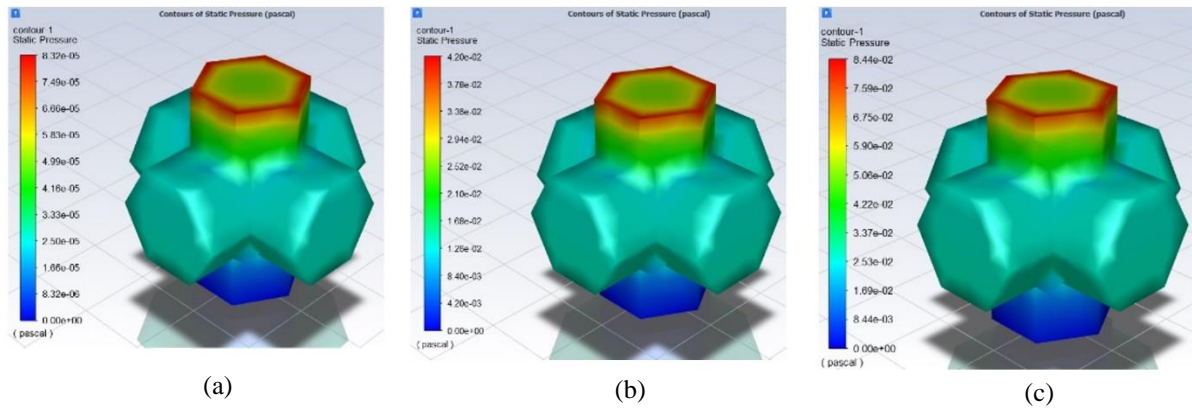


Figure 4. Pressure distribution of 1.5 mm hexagonal unit cell at different velocities (a) 0.001 mm/s, (b) 0.5 mm/s and (c) 1 mm/s

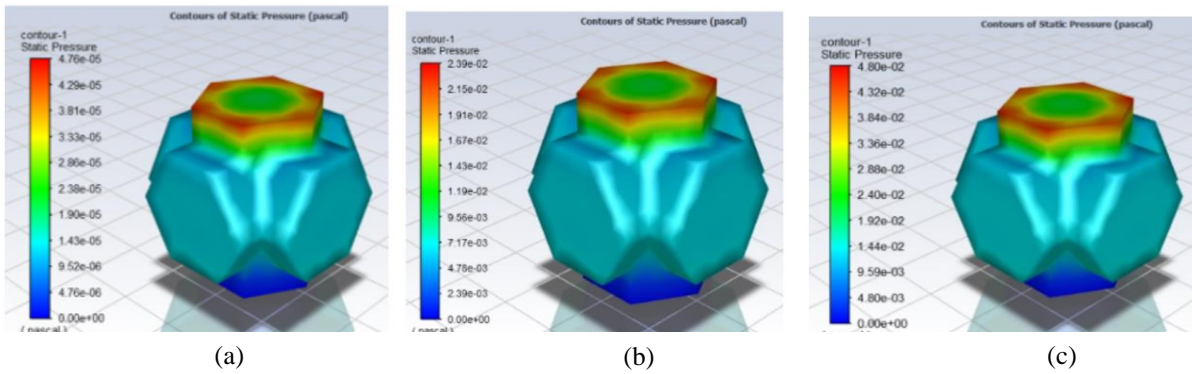


Figure 5. Pressure distribution of 2.0 mm hexagonal unit cell at different velocities (a) 0.001 mm/s, (b) 0.5 mm/s and (c) 1 mm/s

As can be seen in the result of static pressure distribution, for the diameter pores of 1.0 mm, 1.5 mm and 2.0 mm, all scaffolds exhibit similar static pressure distribution. Each model shows higher static pressure at the inlet surface and gradually decreases towards the outlet surface. Figure 6, 7 and 8 shows the pressure distribution at different velocities for 1.0 mm, 1.5 mm and 2.0 mm, respectively.

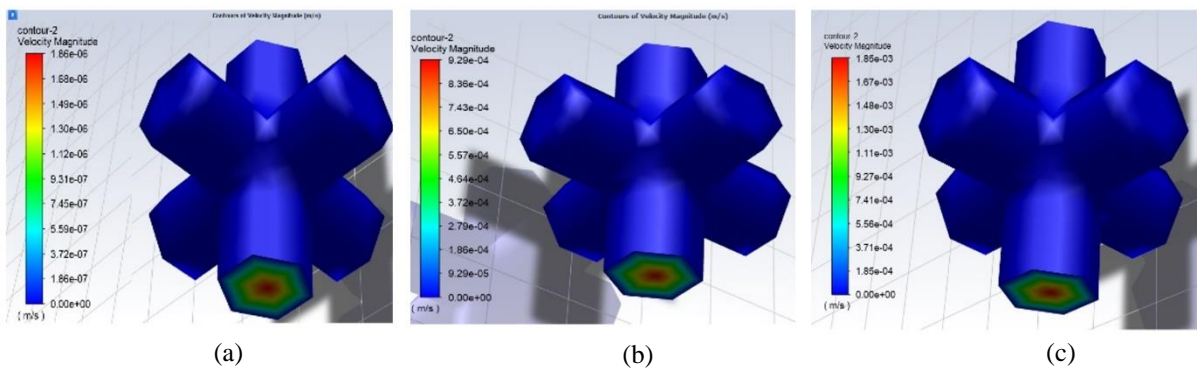


Figure 6. Velocity distribution of 1.5mm hexagonal unit cell at different velocities (a) 0.001 mm/s, (b) 0.5 mm/s and (c) 1 mm/s



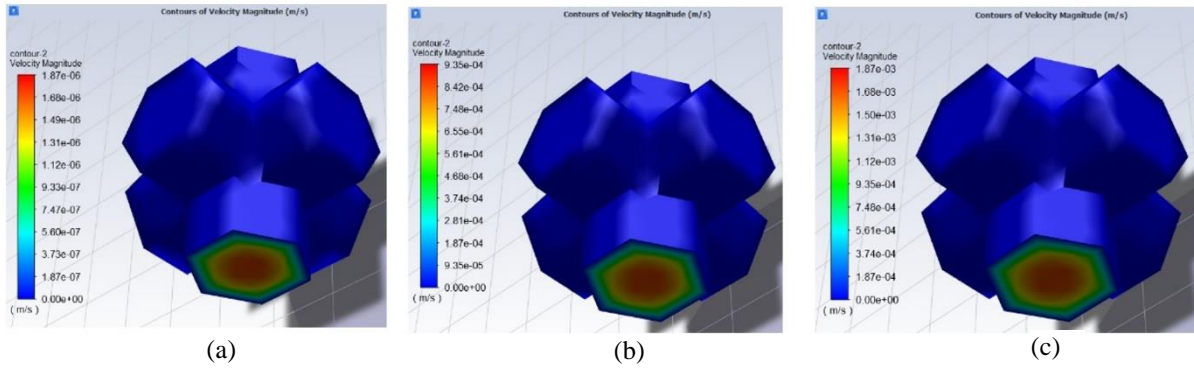


Figure 7. Velocity distribution of 1.5 mm hexagonal unit cell at different velocities (a) 0.001 mm/s, (b) 0.5 mm/s and (c) 1 mm/s

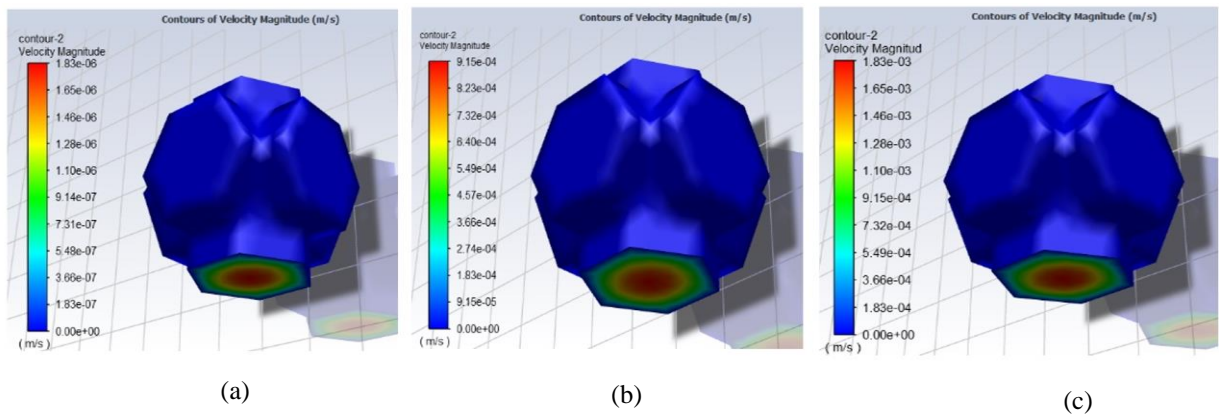


Figure 8. Velocity distribution of 1.5 mm hexagonal unit cell at different velocities (a) 0.001 mm/s, (b) 0.5 mm/s and (c) 1 mm/s

As shown in Figure 6, 7 and 8, the velocity for each pore diameter also shows a similar pattern of distribution. The velocity at the entrance namely the inlet surface structure towards the outlet surface structure of the scaffold is higher while velocity is gradually decreased towards the radial direction originating from the centre pathway. The high velocity in the centre pathway indicates the increase of speed in which it is conducive for cell migration and operating cells to move towards the deepest area of the scaffold [15]. The gradual decrease of velocity towards the internal boundary is favorable for cells and nutrients absorption on the scaffold inner surface [16]. Based on pressure distribution and velocity distribution, pressures drop for hexagonal unit cell at different pore sizes and different velocities are successfully obtained as shown in Table 2 and Figure 5.

Table 2. Pressure drop for hexagonal unit cell at different pore sizes and different velocity

Velocity (mm/s)	Pressure Drop (Pa)		
	Pore size (1.0 mm)	Pore size (1.5 mm)	Pore size (2.0 mm)
0.001	$1.40 \times 10^{-4}$	$8.35 \times 10^{-5}$	$4.76 \times 10^{-5}$
0.5	$7.02 \times 10^{-2}$	$4.20 \times 10^{-2}$	$2.39 \times 10^{-2}$
1	$1.41 \times 10^{-1}$	$8.44 \times 10^{-2}$	$4.80 \times 10^{-2}$

A graphical representation of pressure drop (Pa) versus inlet velocity (mm/s) is plotted based on the simulation result. Pores size of 1 mm shows a higher pressure drop between inlet and outlet surface when inlet velocity is determined at 0.001 mm/s, 0.5 mm/s and 1 mm/s. Based on the result obtained, it can be proved that the pressure drop increased when the pores diameter decreased. The higher-pressure drops leads to the higher flow velocity. By using Darcy’s law, the permeability for each unit cell was successfully calculates, as shown in the Table 3.

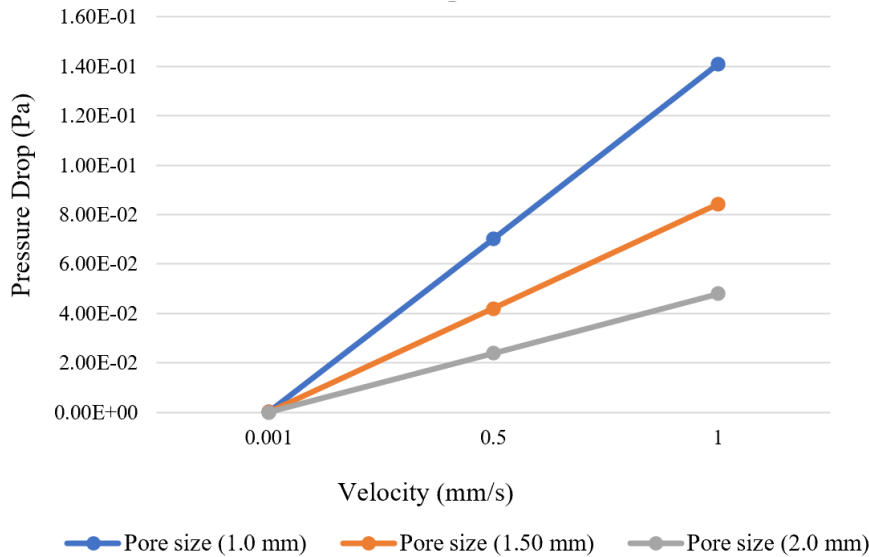


Figure 9. Pressure drop versus inlet velocity for hexagonal unit cell at different pore sizes

Table 3. Permeability of the unit cell results

Velocity (mm/s)	Permeability of Unit Cell (m <sup>2</sup> )		
	Pore size (1.0 mm)	Pore size (1.5 mm)	Pore size (2.0 mm)
0.001	2.900×10 <sup>-8</sup>	4.863×10 <sup>-8</sup>	8.529×10 <sup>-8</sup>
0.5	2.892×10 <sup>-8</sup>	4.833×10 <sup>-8</sup>	8.494×10 <sup>-8</sup>
1	2.879×10 <sup>-8</sup>	4.813×10 <sup>-8</sup>	8.458×10 <sup>-8</sup>

As shown in Table 3, the variation in velocities did not give significant differences for the scaffold permeability. However, the different of pore sizes gave significant effect in the scaffold permeability. From the result in Table 3, the graph permeability versus pore size is successfully plotted, as shown in Figure 10.

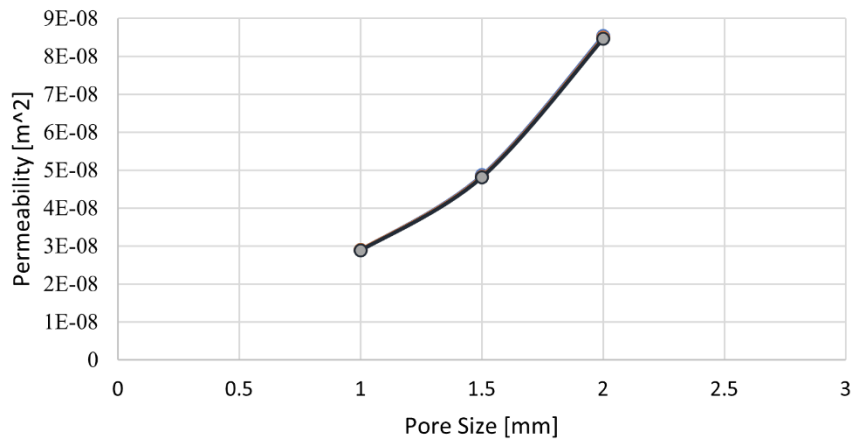


Figure 10. Permeability of hexagonal unit cell at different pore sizes

Figure 10 shows the relationship between the permeability and pore size for hexagonal unit cell. Based on the pressure drop value obtained, permeability of each scaffold is calculated according to the applied inlet velocities. Permeability obtained for each scaffold shows a significant difference between 1.0 mm, 1.5 mm and 2.0 mm pore size. However, the permeability at different velocities shows an insignificant result. The permeability for each scaffold obtained is in the order of 10<sup>-8</sup> at which for 1 mm and 1.5 mm results are acceptable according to the upper limit of human bone permeability (0.5 < k (10<sup>-8</sup>m<sup>2</sup>) < 5) [5]. By taking into account the pressure drops and permeability value, pore size of 1.0 mm shows a better performance to promote cell growth due to the better flow characteristics with highest pressure drop.

Pore properties such as porosity, orientation, size, distribution and interconnectivity are among factors that able to influence the permeability of a scaffolds [17,6]. It is reported that pore interconnectivity influenced the osteogenic and capillary growth which were crucial in bone regeneration [17]. Furthermore, it was also reported that scaffold with higher permeability scaffolds enhanced the bone formation both in-vitro and in-vivo [6,18]. Besides the formation of bone inhibited the formation of cartilage tissue [18]. Generally, adequate pore size provided enough nutrient and oxygen supply for cell growth, proliferation and tissue vascularization [19]. Scaffolds with greater mass transport able to increase bone regeneration since the native bone tissue is highly vascularized [6]. In contrast, scaffold with smaller pore size more suitable in promoting chondrogenesis than bone osteogenesis due to low oxygen tension or hypoxia state [20]. Therefore, permeability needs to be considered as one of important scaffold architecture in developing a successful bone substitute.

#### 4. Conclusion

We have successfully determined the permeability of porous scaffold with different pore sizes. By using various software such as SOLIDWORKS And ANSYS we were able to conduct CFD Simulation to determine various factors such as the pressure drop and inlet velocity. Pressure drop value increased as the pore size decreased. In contrast, increased inlet velocities have increased the pressure drop from inlet to the outlet. However, the changes in velocities did not gave significant differences for the scaffold permeability. However, the different of pore sizes gave significant effect in the scaffold permeability. We concluded that the best permeable scaffolds are the scaffolds with 1 mm and 1.5 mm pore size due to the acceptable permeability value as compared to human bone permeability. Scaffold permeability will affect the osteogenesis and vascularization in bone regeneration. Therefore, good permeability prediction will help in producing a functional bone scaffold that can be utilized as bone substitute in supporting human skeletal function.

#### Acknowledgment

This work was supported by Universiti Teknologi Malaysia and Fundamental Research Grant Scheme (FRGS) grant (FRGS/1/2020/STG05/UTM/02/10) from Ministry of Education, Malaysia.

#### References

- [1] J. Henkel, M. A. Woodruff, D. R. Epari, R. Steck, V. Glatt, I. C. Dickinson, P. F. Choong, M. A. Schuetz and D. W. Hutmacher, Bone regeneration based on tissue engineering conceptions—A 21st century perspective, *Bone Research*, 2013, 1:216–248. <https://doi.org/10.4248/BR201303002>
- [2] M. A. Velasco, C. A. Narváez-Tovar and D. A. Garzón-Alvarado, Design, materials, and mechanobiology of biodegradable scaffolds for bone tissue engineering, *BioMed Research International*, 2015, 2015:1–21. <https://doi.org/10.1155/2015/729076>
- [3] B. Levine, A new era in porous metals: applications in orthopaedics, *Advanced Engineering Material*, 2008, 10(9): 788–792. <https://doi.org/10.1002/adem.200800215>
- [4] M. R. Dias, P. R. Fernandes, J. M. Guedes and S. J. Hollister, Permeability analysis of scaffolds for bone tissue engineering, *Journal of Biomechanics*, 2012, 45(6):938–944. <https://doi.org/10.1016/j.jbiomech.2012.01.019>
- [5] S. P. Singh, M. Shukla and R. K. Srivastava, Lattice modeling and CFD simulation for prediction of permeability in porous scaffolds, *Materials Today: Proceedings*, 2018, 5(9):18879–18886. <https://doi.org/10.1016/j.matpr.2018.06.236>
- [6] A. Mitsak, J. Kemppainen, M. Harris and S. Hollister, Effect of polycaprolactone scaffold permeability on bone regeneration in-vivo, *Tissue Engineering Part A*, 2011, 17(13–14):1831–1839. <https://doi.org/10.1089/ten.tea.2010.0560>
- [7] J. M. Kemppainen, Mechanically stable solid free form fabricated scaffolds with permeability optimized for cartilage tissue engineering. Dissertation. University of Michigan, USA, 2008. <https://hdl.handle.net/2027.42/61582>
- [8] C. G. Jeong, H. Zhang and S. J. Hollister, Three-dimensional poly (1,8-octanediol– co-citrate) scaffold pore shape and permeability effects on sub-cutaneous in vivo chondrogenesis using primary chondrocytes, *Acta Biomaterialia*, 2011, 7(2):505–514. <https://doi.org/10.1016/j.actbio.2010.08.027>
- [9] S. Li, J. R De Wijn, J. Li, P. Layrolle and K. De Groot, Macroporous biphasic calcium phosphate scaffold with high permeability/porosity ratio, *Tissue Engineering*, 2003, 9(3):535–548. <https://doi.org/10.1089/107632703322066714>
- [10] K. W. Lee, S. Wang, L. Lu, E. Jabbari, B. L. Currier and M. J. Yaszemski, Fabrication and characterization of poly (propylene fumarate) scaffolds with controlled pore structures using 3-dimensional printing and injection molding, *Tissue Engineering*, 2006, 12(10):2801–2811. <https://doi.org/10.1089/ten.2006.12.2801>



- [11] M. V. Chor and W. Li, A permeability measurement system for tissue engineering scaffolds, *Measurement Science and Technology*, 2006, 18(1):208–216. <https://doi.org/10.1088/0957-0233/18/1/026>
- [12] A. M. Grumezescu, *Nanobiomaterials in Soft Tissue Engineering: Application of Nanobiomaterials*, 1st ed., United States: William Andrew Publishing, 2016.
- [13] T. Ghassemi, A. Shahroodi, M. H. Ebrahimzadeh, A. Mousavian, J., Movaffagh and A. Moradi, Current concepts in scaffolding for bone tissue engineering, *The Archives of Bone and Joint Surgery*, 2018, 6(2):90–99. <https://dx.doi.org/10.22038/abjs.2018.26340.1713>
- [14] S. Truscello, G. Kerckhofs, S. Van Bael, G. Pyka, J. Schrooten and H. Van Oosterwyck, Prediction of permeability of regular scaffolds for skeletal tissue engineering: a combined computational and experimental study, *Acta Biomaterialia*, 2012, 8(4):1648–1658. <https://doi.org/10.1016/j.actbio.2011.12.021>
- [15] S. Wang, L. Liu, X. Zhou, L. Zhu and Y. Hao, The design of Ti6Al4V primitive surface structure with symmetrical gradient of pore size in biomimetic bone scaffold, *Materials & Design*, 2020, 193:108830. <https://doi.org/10.1016/j.matdes.2020.108830>
- [16] C. Wang, Y. Zhou, L. He, Z. Chen and S. Tian, 3D printing of bone tissue engineering scaffolds, *Bioactive Materials*, 2020, 5(1):82–91. <https://doi.org/10.1016/j.bioactmat.2020.01.004>
- [17] N. Abbasi, S. Hamlet, R.M. Love and N.T. Nguyen, Porous scaffolds for bone regeneration. *Journal of Science: Advanced Materials and Devices*, 2020, 5(1);1–9. <https://doi.org/10.1016/j.jsamd.2020.01.007>
- [18] G. Turnbull, J. Clarke, F. Picard, P. Riches, L. L. Jia, F. X. Han, B. Li and W. M. Shu, 3D bioactive composite scaffolds for bone tissue engineering, *Bioactive Materials*, 2018 3(3):278–314. <https://doi.org/10.1016/j.bioactmat.2017.10.001>
- [19] Y. Q. Kang and J. Chang, Channels in a porous scaffold: A new player for vascularization, *Regenerative Medicine*, 2018, 13(6):704–715. <https://doi.org/10.2217/rme-2018-0022>
- [20] T. H. Lin, H. C. Wang, W. H. Cheng, H. C. Hsu and M. L. Yeh, Osteochondral tissue regeneration using a tyramine-modified bilayered PLGA scaffold combined with articular chondrocytes in a porcine model, *International Journal of Molecular Science*, 2019, 20(2):326. <https://doi.org/10.3390/ijms20020326>